

Influence of Dofour and Soret on Eyring-Powell Nanofluid Flow from A Circular Cylinder with Viscous Dissipation

Khaled K. Jaber

Abstract — The impact of Viscous dissipation on the heat and mass transfer characteristics of an Eyring Powell nanofluid flow past a horizontal circular cylinder is intensively investigated in the presence of Dufour and Soret effects. The free laminar flow is subject to a uniform transverse magnetic field. The continuity, momentum, energy, and concentrations equations are transformed into a nonlinear system of partial differential equations using appropriate non-similarity variables. The transformed system was solved numerically using the fourth order Runge Kutta method. The effect of parameters including Prandtl number, Dufour effect, Soret effect and Schmidt number were studied and presented graphically. Nusselt and Sherwood numbers have also been derived and discussed numerically.

Keywords —Eyring-Powell fluid; Soret and Dufour effects; viscous dissipation.

I. INTRODUCTION

Convection heat transfer in a flow through porous medium is a widespread phenomenon of great interest due to its fundamentally important applications in geothermal and petroleum resources, heat exchanger, geophysical, engineering and environmental fields. Also, they have a great importance in boiling enhancement, insulation and compact heat exchanger. Furthermore, free convection in channel flow has many important applications in designing ventilating and heating of buildings, cooling of electronic components of a nuclear reactor, bed thermal storage, and heat sink in the turbine blades. Free convection flows past a semi-infinite vertical plate under different physical conditions have been studied by [1]. Reference [2] studied the effect of Hall currents, radiation and variable viscosity on free convective flow past a semi-infinite continuously stretching plate, [3] studied the effect of Hall currents and variable fluid properties on MHD flow past a continuously stretching vertical plate in the presence of radiation. Due to the important role of Viscous dissipation in natural convection in processes subjected to big contrast of gravitational force or devices which operate at high speeds, viscous dissipation effect on MHD flow attracted the interest of many researchers. Reference [4] examined the effects of viscous dissipation and joule heating on MHD flow of a fluid with variable properties past a stretching vertical plate. The prefix ‘nano’ is a prefix meaning something very small and depicts one thousand millionth of a meter (10^{-9} m). In 1959 the Nobel prize laureate Richard Feynman introduced the nanometer concept during his lecture in the annual meeting of the American Physical Society. Nanofluid is a fluid which contains nanometer-sized particles typically made of nanofibers metals or oxides and so on. The first who studied nanofluid flow was [5] in 1995, he studied the thermal conductivity of the fluid contains nanoparticles, he established that adding less than 1% nanoparticles to the base fluid can increase the thermal conductivity. Since that nanofluid attracted the attention of many researchers due to the important role in enhancing the thermal and mass flow in industrial and engineering processes. The diffusion thermo effect “Dufour” is the energy flux produced by a concentration gradient. On the other hand, the temperature gradient can cause mass flux which is the thermal diffusion or Soret effect. In spite of the small effect of Soret and Dufour effects in heat and mass transfer they have a considerable effect in many processes, The Soret effect has been used in forisotope separation and in mixing very small molecular weight gases like Hydrogen a Helium. The Dufour effect has been used in mixtures of gasses with larger molecular weight like Nitrogen and air. Reference [6] investigated the effect of thermal-diffusion and diffusion-thermo effects on free convection heat and mass transfer in an electrically conducting non-Darcy fluid. Reference [7] investigate the Soret and Dufour effects on mixed convective fluid flow past a vertical porous plate with variable suction. Further, [8] studied the Dufour and Soret effects on free convection flow of a non-Darcy fluid adjacent to a vertical plate with temperature dependent viscosity. Albert Einstein in 1905 produce his quantitative theory of Brownian motion in light of the Brownian theory “the temperature of a substance is proportional to the average kinetic energy with which the molecules of the substance are moving or vibrating”. Reference [9] showed that Thermophoresis and Brownian motion are the most important sliding motion of nanoparticles in a base

fluid with a relative velocity. Based on the result of [10] proved that the Nusselt number increases with the decreasing of each Nr , Nb and Nt parameters. Reference [11] analyzed the attractive procedure for cooling nanofluid using a new Lattice-Boltzmann. References [12]-[15] explained the effects of Brownian motion and thermophoresis on nanofluids flow over a stretching sheet. Eyring-Powell fluid is a generalized non-Newtonian fluid, they do not follow Newton's law of viscosity. The constitutive equation of the generalized non-Newtonian fluid which is non-Newtonian fluid is a generalized form of Newton's law. There are many researches to study the behavior of non-Newtonian fluids. Reference [16] analyzed the Combined Effects of Hall Current and Variable Viscosity on Non-Newtonian MHD Flow Past a Stretching Vertical Plate. Reference [17] perform a computational study of Eyring-Powell fluid flow near a horizontal circular cylinder with biot number effect. Reference [18] studied non-Newtonian thermal convection from an isothermal sphere with piot number effect. Reference [19] perform a computational study of non-Newtonian Eyring-Powell fluid from a vertical porous plate with piot number effect. Reference [20] analyzed the heat transfer of a Darcy Nanofluid MHD flow over a stretching/shrinking surface Reference [21] study the Darcy-Forchheimer flow of hybrid nanoparticles flow over a permeable stretched cylinder. Plenty theoretical and computational works concern on flow from cylindrical bodies, which appear in polymer processes. Reference [22] presented an early analysis of heat transfer in flow over a slender cylinder, they showed that transverse bending has a strong effect on skin friction at medium and large distances from the leading edge of the boundary layer. Reference [23] demonstrated the heat flow of a non-Newtonian fluid on circular cylinder and spherical bodies using the Merk-Chao series solution method. Reference [24] studied Newtonian heating in Williamson non-Newtonian fluid flow around a circular cylinder. Reference [25] researched the thermal Radiation Effects on Old royd-B Nano fluid from a Stretching Sheet in a non-Darcy porous medium. For more reading, see the following references [26]-[32].

In the present work, a mathematical model is presented to study the MHD free convection boundary layer flow in an Eyring-Powell fluid past a circular cylinder. The governing equations transformed to a system of dimensionless partial differential equations subjected to physical boundary conditions, which in turns solved numerically using the fourth order Runge Kutta method. The involved parameters i.e. Prandtl number Pr , magnetic parameter M , Schmidt number Sc , Grashof number Gr , Eyring-Powell fluid parameter ϵ , Soret coefficient Sr , Dufour coefficient Du , Brownian motion parameter Nb and thermophoresis parameter Nt are investigated and illustrated graphically. Also, the effect of the involved parameters on skin friction and Nusselt number have been studied and tabulated.

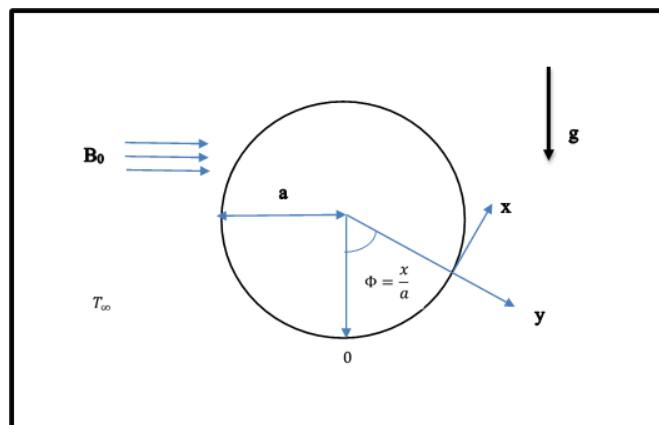


Fig. 1. Physical model and coordinates.

II. MATHEMATICAL FORMULATION

The steady two-dimensional laminar flow of mass and heat transfer in an incompressible electrically conducted Eyring-Powell nanofluid over a circular cylinder is investigated. The physical situation of the problem under consideration is depicted as in Fig. 1. The x -coordinate is measured from the lowest point, along the circumference of the cylinder, the y -axis is taken perpendicular to the surface. The angle of the y -axis with respect to the vertical equal $\Phi = \frac{x}{a}$ where $0 \leq \Phi \leq \pi$. The Boussineq approximation holds, and the Reynold's number is taken to be small enough (as in laminar flow $Re < 2100$) so the induced magnetic field can be neglected. Initially the cylinder and the Eyring-Powell nanofluid are maintained at the same temperature, then the temperature raised to $T_w > T_\infty$. In view of [24] and the taken boundary layer approximations.

The governing equations can be written as:

$$\frac{\partial u}{\partial \bar{x}} + \frac{\partial v}{\partial \bar{y}} = 0 \tag{1}$$

$$\frac{\partial u}{\partial \bar{x}} + v \frac{\partial u}{\partial \bar{y}} = \left(v + \frac{1}{\rho_f \beta c} \right) \frac{\partial^2 u}{\partial \bar{y}^2} - \frac{1}{2\rho_f \beta c^3} \left(\frac{\partial u}{\partial \bar{y}} \right)^2 \frac{\partial^2 u}{\partial \bar{y}^2} - \frac{\sigma B_0^2 u}{\rho_f} \tag{2}$$

$$u \frac{\partial T}{\partial \bar{x}} + v \frac{\partial T}{\partial \bar{y}} = \alpha \frac{\partial^2 T}{\partial \bar{y}^2} + \frac{(\rho c)_p}{(\rho c)_f} D_B \left[\frac{\partial T}{\partial \bar{y}} \frac{\partial C}{\partial \bar{y}} \right] + \frac{D_B K_T}{C_s C_p (\rho c)_f} \left(\frac{\partial^2 C}{\partial \bar{y}^2} \right) + \frac{(\rho c)_p}{(\rho c)_f} \frac{D_B K_T}{T_m} \left(\frac{\partial T}{\partial \bar{y}} \right)^2 \tag{3}$$

$$u \frac{\partial C}{\partial \bar{x}} + v \frac{\partial C}{\partial \bar{y}} = D_B \frac{\partial^2 C}{\partial \bar{y}^2} + \frac{D_B K_T}{T_m} \frac{\partial^2 T}{\partial \bar{y}^2} \tag{4}$$

where u is the velocity component along the cylinder and v is the transvers component, ν is the kinematic viscosity of the nanofluid, β is the non-Newtonian Eyring parameter, α is the thermal diffusivity, T is the temperature, K is the permeability coefficient of the porous medium, T_∞ is the temperature of the ambient fluid. The physical regime suggested the following boundary conditions at the circulation and the edge of the boundary layer as follows:

$$\begin{aligned} u = u_w, v = -v_w, T = T_w & : \text{as } y = 0 \\ u \rightarrow 0, T \rightarrow T_\infty & : \text{as } y \rightarrow \infty \end{aligned} \tag{5}$$

In order to reduce the previous system consists of Equations (1)-(4) subjected to the boundary conditions (5) to a convenient non-dimensional form the following dimensionless quantities are introduced:

$$x = \frac{\bar{x}}{a}, y = \frac{\bar{y}}{a} Gr^{\frac{1}{4}}, \psi = v \frac{\bar{x}}{a} Gr^{\frac{1}{4}} f(\bar{x}, \bar{y}), \theta = \frac{T - T_\infty}{T - T_w}, \phi = \frac{C - C_\infty}{C - C_w}, qr = \frac{-16\sigma^* T_\infty^3}{3K^*} \frac{\partial T}{\partial \bar{y}}$$

where the stream function ψ satisfying the continuity equation $u = \frac{\partial \psi}{\partial \bar{x}}$ and $v = -\frac{\partial \psi}{\partial \bar{y}}$

In view of the previous dimensionless quantities Equations (1)-(4) reduced to the following system of non-dimensional partial differential equations:

$$\begin{aligned} f'^2 + x \left(f' \frac{\partial f'}{\partial x} - f'' \frac{\partial f}{\partial x} \right) - f f'' \\ = (1 + \epsilon) f'''' - \epsilon \delta x^2 f''^2 f'''' - \frac{M}{\sqrt{Gr}} f' \end{aligned} \tag{6}$$

$$\begin{aligned} + \frac{\sin x}{x} \left(\theta + \frac{Gr c}{Gr} \phi \right) \\ x f' \frac{\partial \theta}{\partial x} - \theta' \left(f + x \frac{\partial f}{\partial x} \right) = \frac{1}{Pr} \theta'' + Nb \theta' \phi' + Du \phi'' + Nt \theta'^2 \end{aligned} \tag{7}$$

$$\frac{1}{Sc} \phi'' + Sr \theta'' + f \frac{\partial \phi}{\partial y} = x \left(f' \frac{\partial \phi}{\partial x} - \phi' \frac{\partial f}{\partial x} \right) \tag{8}$$

where prime denotes differentiation with respect to y . Also, the boundary conditions are transformed to the following non-dimensional form

$$\begin{aligned} f = f' = 0, \theta = \phi = 1 \text{ at } y = 0 \\ f' \rightarrow 0, \theta \rightarrow 0 \text{ and } \phi \rightarrow 0 \text{ as } y \rightarrow \infty \end{aligned} \tag{9}$$

Where $Gr = \frac{g\beta a^3 (T_w - T_\infty)}{\nu^2}$ is the Grashof number, $Gr c = \frac{g\beta a^3 (C_w - C_\infty)}{\nu^2}$ is the concentration Grashof number. $\delta = \frac{\nu^2 Gr^{\frac{3}{2}}}{2a^4}$, $M = \frac{\sigma B_0^2 a^2}{\rho_f \nu}$ is the magnetic field parameter, $\epsilon = \frac{1}{\nu \rho_f \beta c}$ is Eyring-Powell fluid parameter, $Du = \frac{D_B K_T (C_w - C_\infty)}{C_s C_p \nu (T_w - T_\infty)}$ is the Dufour coefficient, $Sr = \frac{D_B K_T (T_w - T_\infty)}{T_m \nu (C_w - C_\infty)}$ is the Soret coefficient, where $D_B = \frac{KTC}{3\pi \mu d_p}$, $N_t = \frac{RD_T (T_w - T_\infty)}{T_m \nu}$ is the thermophoresis parameter, $N_b = \frac{RD_B (C_w - C_\infty)}{\nu}$ is the Brownian motion parameter, $R = \frac{(\rho c)_p}{(\rho c)_f}$ is the ratio effective heat capacity, $Sc = \frac{D_B}{\nu}$ is the Schmidt number. The engineering quantities of physical interest namely, the skin friction coefficient which is the resistant force acting on a particle moving in a fluid, Nusselt number and Sherwood number are specified as:

$$C_f = \frac{2\tau}{\rho u^2} = \frac{2\mu}{\rho u^2} \left. \frac{\partial u}{\partial y} \right|_{y=0} \tag{10}$$

$$= Gr^{\frac{3}{4}} \left[(1 + \epsilon) x f''(x, 0) - \frac{\epsilon \delta}{3} (x f''(x, 0))^3 \right] \tag{11}$$

$$Nu = \frac{\text{Heat transfer by Convection}}{\text{Heat transfer by conduction}} = -Gr^{\frac{1}{4}} \theta'(x, 0) \tag{12}$$

$$Sh = \frac{\text{Convection mass transfer rate}}{\text{Diffusion rate}} = -Gr^{\frac{1}{4}} \phi'(x, 0)$$

TABLE I: VARIATION OF THE DIMENSIONLESS SKI FRICTION AND LOCAL NUSSELT NUMBER FOR VARIOUS PARAMETERS WITH P=0.5 AND PR=0.7 FOR (PST) CASE

| M | ϵ | Du | Gr | Grc | Nb | Nt | Sc | Sr | $f''(x, 0)$ | $-\theta'(x, 0)$ | $\phi'(x, 0)$ |
|---|------------|-----|------|-----|-----|-----|------|-----|-------------|------------------|---------------|
| 1 | 1 | 0.1 | 1 | 1 | 0.5 | 0.5 | 0.25 | 0.5 | 0.80014 | 0.2771864 | -0.2955637 |
| 4 | 1 | 0.1 | 1 | 1 | 0.5 | 0.5 | 0.25 | 0.5 | 0.565043 | 0.235517 | -0.280585 |
| 7 | 1 | 0.1 | 1 | 1 | 0.5 | 0.5 | 0.25 | 0.5 | 0.459104 | 0.217718 | -0.274471 |
| 1 | 4 | 0.1 | 1 | 1 | 0.5 | 0.5 | 0.25 | 0.5 | 0.416303 | 0.238541 | -0.281837 |
| 1 | 8 | 0.1 | 1 | 1 | 0.5 | 0.5 | 0.25 | 0.5 | 0.258961 | 0.216953 | -0.274289 |
| 1 | 1 | 2 | 1 | 1 | 0.5 | 0.5 | 0.25 | 0.5 | 0.816532 | 0.225611 | -0.303778 |
| 1 | 1 | 6 | 1 | 1 | 0.5 | 0.5 | 0.25 | 0.5 | 0.882822 | 0.0059719 | -0.337241 |
| 1 | 1 | 0.1 | 0.15 | 1 | 0.5 | 0.5 | 0.25 | 0.5 | 2.22215 | 0.387171 | -0.340101 |
| 1 | 1 | 0.1 | 35 | 1 | 0.5 | 0.5 | 0.25 | 0.5 | 0.529176 | 0.252546 | -0.286772 |
| 1 | 1 | 0.1 | 1 | 0.1 | 0.5 | 0.5 | 0.25 | 0.5 | 0.470153 | 0.238923 | -0.281883 |
| 1 | 1 | 0.1 | 1 | 0.3 | 0.5 | 0.5 | 0.25 | 0.5 | 0.545369 | 0.247998 | -0.285067 |
| 1 | 1 | 0.1 | 1 | 1 | 3 | 0.5 | 0.25 | 0.5 | 0.843146 | 0.112739 | -0.320146 |
| 1 | 1 | 0.1 | 1 | 1 | 6 | 0.5 | 0.25 | 0.5 | 0.877385 | 0.0273236 | -0.334822 |
| 1 | 1 | 0.1 | 1 | 1 | 0.5 | 1 | 0.25 | 0.5 | 0.809997 | 0.236941 | -0.301468 |
| 1 | 1 | 0.1 | 1 | 1 | 0.5 | 2 | 0.25 | 0.5 | 0.827408 | 0.178291 | -0.310574 |
| 1 | 1 | 0.1 | 1 | 1 | 0.5 | 0.5 | 2 | 0.5 | 0.737509 | 0.234751 | -0.55933 |
| 1 | 1 | 0.1 | 1 | 1 | 0.5 | 0.5 | 4 | 0.5 | 0.701383 | 0.211061 | -0.777414 |
| 1 | 1 | 0.1 | 1 | 1 | 0.5 | 0.5 | 0.25 | 5 | 0.949047 | 0.392696 | 0.20433 |
| 1 | 1 | 0.1 | 1 | 1 | 0.5 | 0.5 | 0.25 | 20 | 1.06625 | 0.511997 | 0.933663 |

III. RESULTS AND DISCUSSION

Equation (6)-(8) with boundary conditions (9), are solved numerically using Mathematica software to run the fourth-order Runge-Kutta method algorithm by the shooting technique. The value of y at infinity is fixed at 4; the requirement that the variation of velocity and temperature distribution is less than 10^{-9} between any two successive iteration is employed as the criterion of convergence. Fig. 2 and 3 show the effect of the Magnetic Number M on the flow velocity within the boundary layer. It is seen that increasing the magnetic number M decreases the dimensionless velocity f' and increases the temperature of the liquid. Increasing the magnetic field enhances the Lorentz forces acting in the opposite direction to the flow, impeding the flow, causing the temperature to rise. Fig. 4 and 5 established the influence of the Eyring-Powell fluid parameter ϵ . Velocity decreased with increasing values of Eyring-Powell parameter owing to the drop in viscosity at large distance from the cylinder. On the contrary, the temperature transfer is improved with increasing values of ϵ . The variation of values of ϵ slightly affect the concentration so, the Figure is not presented. The impact of the Dufour coefficient Du on velocity, temperature and concentration profiles is presented in Fig. 6-8. Fig. 6 and 7 clearly show that increasing the Dufour coefficient Du increases both velocity and temperature, while it is evident from Fig. 8 that concentration decreases with an increase in values of Dufour coefficient Du . Fig. 9-11 are plotted to study the effect of Grashof number on velocity, heat and mass transfer profiles. It is perceived that Grashof number, which is the quotient of buoyant forces to viscous forces, has a significant effect in this study due to the assumption that Reynold's number Re is small. Fig. 9 reveals that the flow velocity decreased to the increase in the Grashof number, Fig. 10 and 11 show that temperature and mass transfer increase with the increase in Gr . The impression of rising the concentration Grashof number is traded in Fig. 12 and 13. It is noticed that the ascending values of Grc leads to enhance the temperature flow and to decrease the mass flow as shown in Fig. 12 and 13 respectively. Fig. 14-16 demonstrate the influence of the Brownian motion parameter Nb . Growing values of Nb leads to an increase in velocity and temperature of the nanofluid as shown in Fig. 14 and 15 respectively. An increase in Nb leads to an increase in the collision between fluid molecules which in turn leads to an increase in the temperature. Fig. 16 demonstrated that mass concentration of nanoparticles decreases with an increase in Nb parameter. The thermophoresis parameter Nt has the same effect as Brownian parameter as shown in Fig. 17-19. By comparing Fig. 16 with Fig. 19 it is clearly that Brownian parameter has greater effect in reducing mass flow. Schmidt number is the ratio of momentum diffusivity

and mass diffusivity it describes mass transfer. Fig. 20 and 21 illustrated to analyze the effect of Schmidt number on velocity and nanoparticles concentration distribution, it is clearly noticed that an increase of Schmidt number leads to decrease both velocity and concentration diffusivity. Fig. 22-24 illustrated the impact of Soret coefficient Sr . The mounting Soret coefficient enhances the flow velocity and mass concentration flow. On the other hand the temperature decrease due to the increase in Sr .

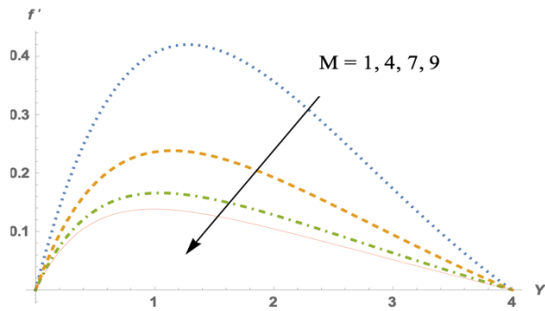


Fig. 2. Velocity profiles for different values of M .

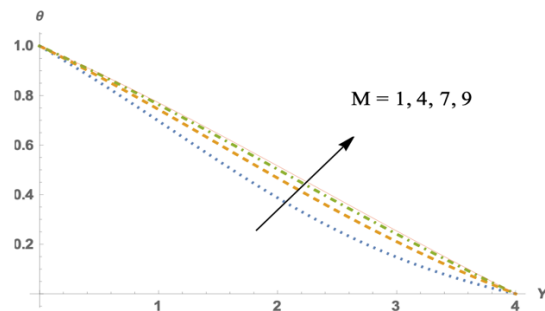


Fig. 3. Temperature profiles for different values of M .

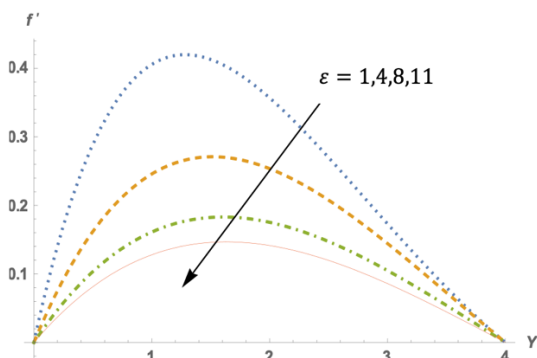


Fig. 4. Velocity profiles for different values of ϵ .

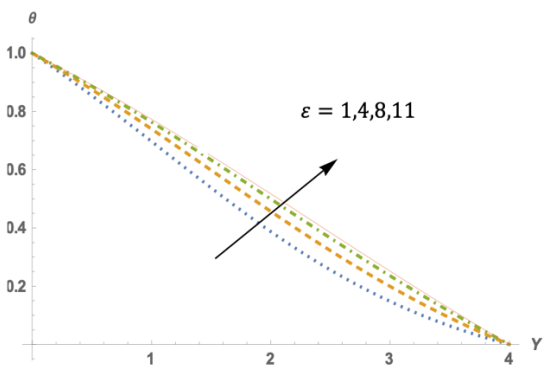


Fig. 5. Temperature profiles for different values of ϵ .

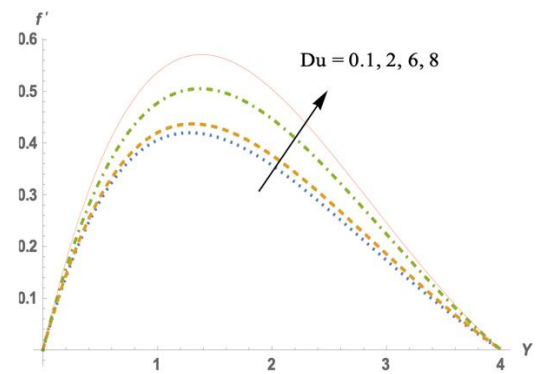


Fig. 6. Velocity profiles for different values of Du .

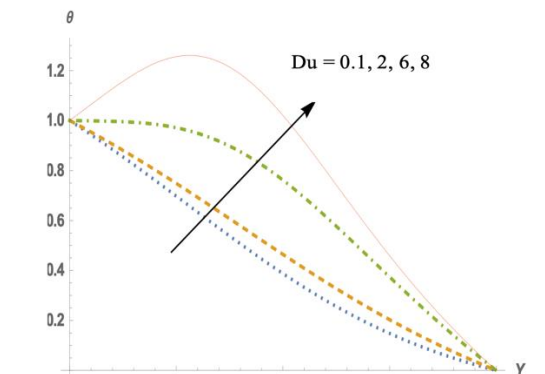


Fig. 7. Temperature profiles for different values of Du .

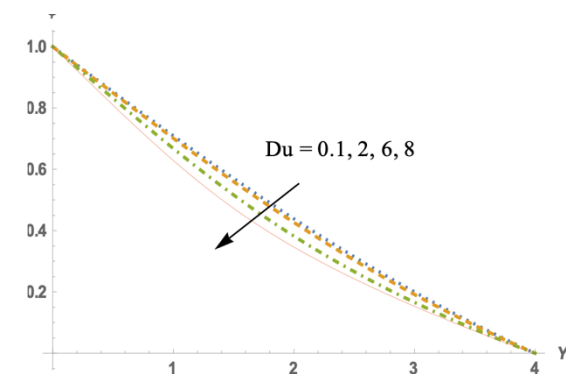


Fig. 8. Concentration profiles for different values of Du .

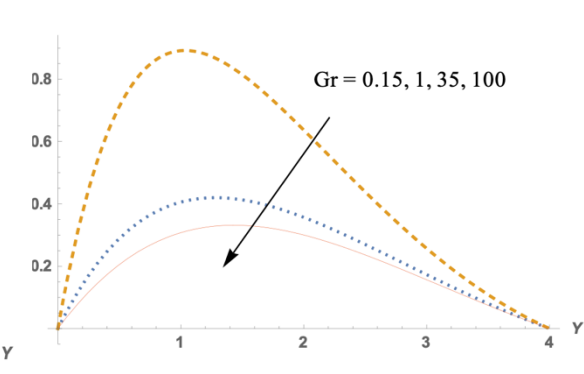


Fig. 9. Velocity profiles for different values of Gr .

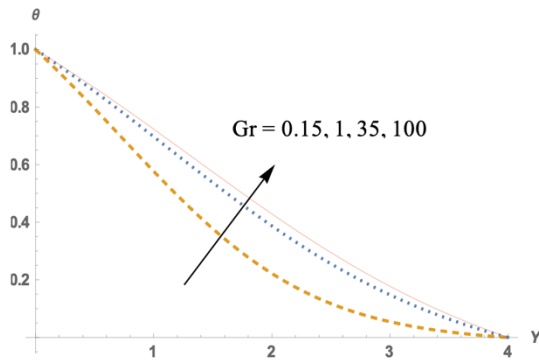


Fig. 10. Temperature profiles for different values of Gr.

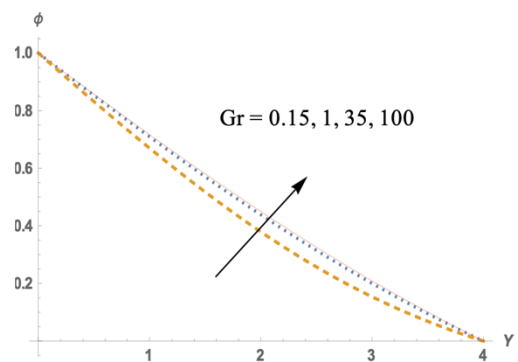


Fig. 11. Concentration profiles for different values of Gr.

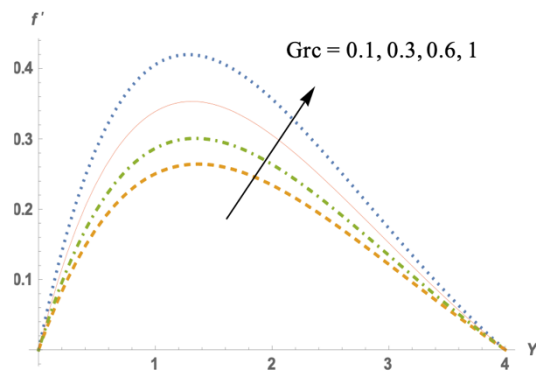


Fig. 12. Velocity profiles for different values of Grc.

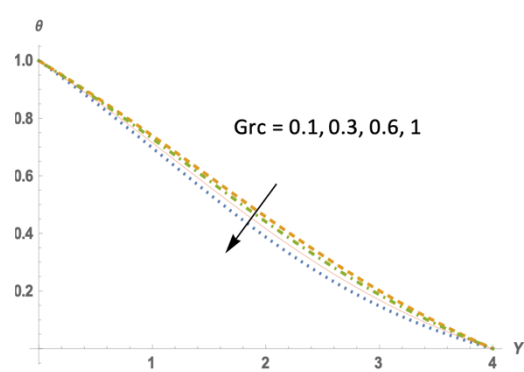


Fig. 13. Temperature profiles for different values of Grc.

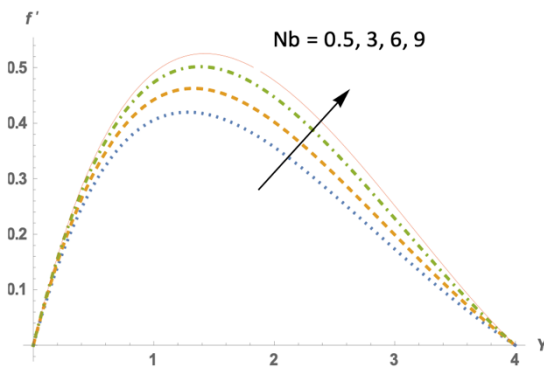


Fig. 14. Velocity profiles for different values of Nb.

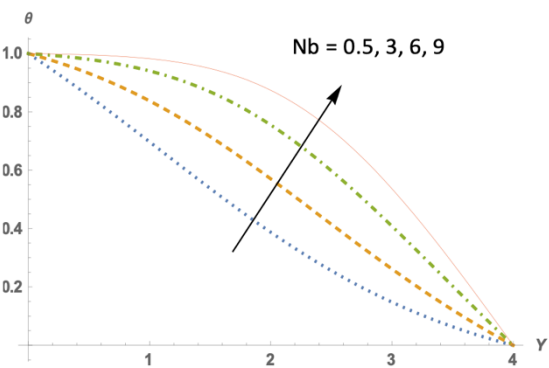


Fig. 15. Temperature profiles for different values of Nb.

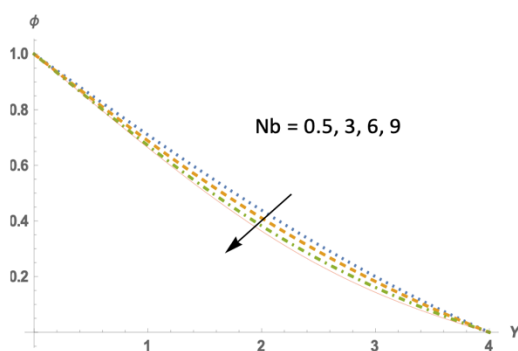


Fig. 16. Concentration profiles for different values of Nb.

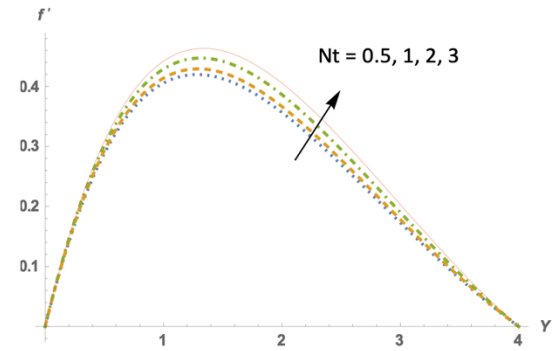


Fig. 17. Velocity profiles for different values of Nt.

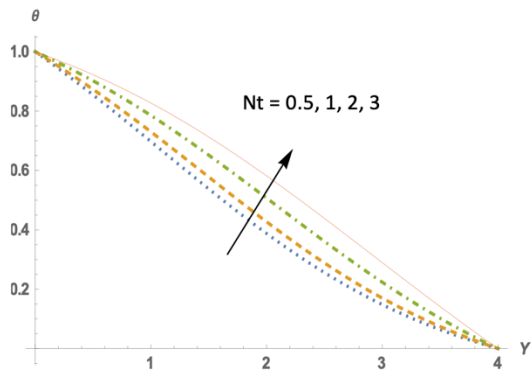


Fig. 18. Temperature profiles for different values of Nt .

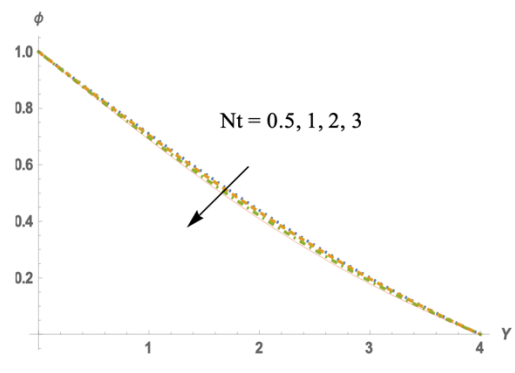


Fig. 19. Concentration profiles for different values of Nt .

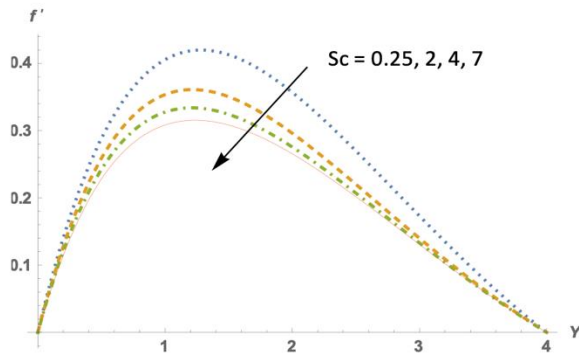


Fig. 20. Velocity profiles for different values of Sc .

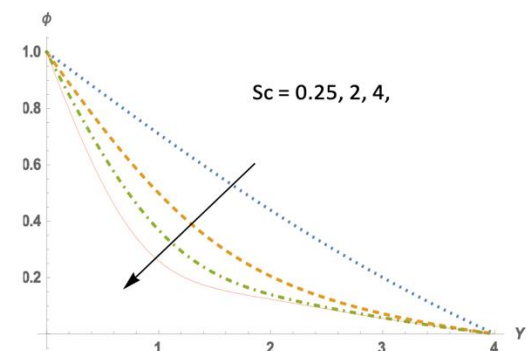


Fig. 21. Concentration profiles for different values of Sc .

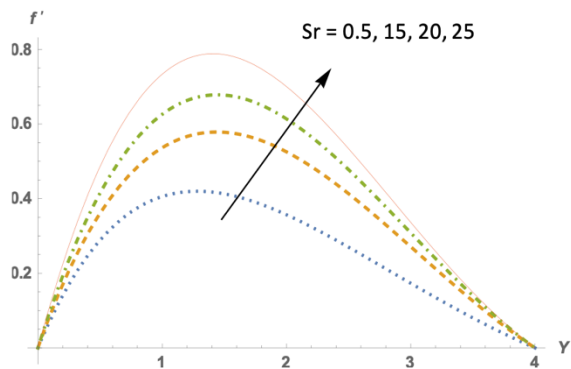


Fig. 22. Velocity profiles for different values of Sr .

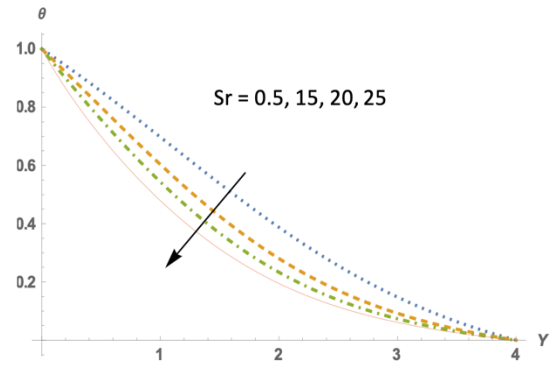


Fig. 23. Temperature profiles for different values of Sr .

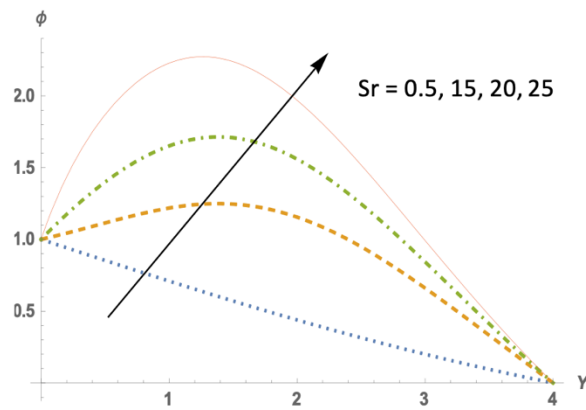


Fig. 24. Concentration profiles for different values of Sr .

IV. CONCLUSION AND REMARKS

The aim of the present study is to investigate heat and mass transfer on steady and laminar flow of a non-Newtonian Eyring-Powell fluid subjected to a uniform transverse magnetic field. The fluid flow past a permeable horizontal circular cylinder embedded in a non-Darcy porous medium. Using appropriate non-dimensional quantities and boundary layer assumptions the equations of the Mathematical modeling transformed to a system of partial differential equations subject to realistic boundary conditions. The fourth order Runge-Kutta method has been utilized to efficiently solve the transformed system. The computations shown that:

1. The flow velocity increased due to the increase in Dufour coefficient Du , concentration Grashof number Gr_c , Dufour coefficient Sr , Brownian motion parameter Nb and thermophoresis parameter Nt , while escalating values of magnetic number M , Eyring-Powell fluid parameter ϵ , Grashof Gr and Schmidt number Sc reduce the velocity in the boundary layer.
2. The temperature improved due to the increase in the value of the magnetic number M , Eyring-Powell fluid parameter ϵ , Schmidt number Sc , Grashof Gr , Dufour coefficient Du , Brownian motion parameter Nb and thermophoresis parameter Nt . Growing values of concentration Grashof number Gr_c and Soret coefficient Sr tend to depress the temperature.
3. The concentration field increased with the increase in magnetic number M , Grashof number Gr , Eyring-Powell fluid parameter ϵ and Soret coefficient Sr , whereas the concentration field decreased due to the increase in Schmidt number Sc , Dufour coefficient Du , Brownian motion parameter Nb and thermophoresis parameter Nt .
4. The skin friction increased by increasing concentration Grashof number Gr_c , Soret coefficient Sr , Brownian motion parameter Nb and thermophoresis parameter Nt , whereas it is decreased due to the increase in magnetic number M , Grashof number Gr , Eyring-Powell fluid parameter ϵ , Dufour coefficient Du and Schmidt number Sc .
5. The Nusselt number increased owing to the increase in magnetic number M , Eyring-Powell fluid parameter ϵ , Dufour coefficient Du , Grashof number Gr , Brownian motion parameter Nb , and Schmidt number Sc . The Nusselt number decreased by increasing concentration Grashof number Gr_c , thermophoresis parameter Nt and Soret coefficient Sr .
6. The Sherwood number increased by the growing the values of magnetic number M , Grashof number Gr , Eyring-Powell fluid parameter ϵ , and Soret coefficient Sr , whereas it is decreased owing to the decreased in Dufour coefficient Du , concentration Grashof number Gr_c , Brownian motion parameter Nb and thermophoresis parameter Nt and Schmidt number Sc .

REFERENCES

- [1] E. Pohlhausen: Der Wärmeaustausch Zwischen Festen Korpen und Flüssigkeiten mit Kleiner Reibung und kleiner Wärmeleitung. *ZAMM*. 1921; 1: 115-121. German.
- [2] Jaber KK. Effect of Hall currents and variable fluid properties on MHD flow past stretching vertical plate by the presence of radiation. *Journal of Applied Mathematics and Physics*. 2014; 2: 888-902.
- [3] Jaber KK. Combined effects of Hall current and variable viscosity on Non-Newtonian MHD flow past a stretching vertical plate. *Journal of Advances in Mathematics*. 2014; 7(3).
- [4] Jaber KK. Effect of viscous dissipation and Joule heating on MHD flow of a fluid with variable properties past a stretching vertical plate. *European Scientific Journal*. 2014; 10(33).
- [5] Choi SU, Eastman JA. Enhancing thermal conductivity of fluids with nanoparticles. Argonne National Lab., IL (United States). 1995.
- [6] Partha MK, Murthy PVS, Sekhar GPR. Soret and Dufour effects in a non-Darcy porous medium. *Journal of Heat Transfer*. 2006; 128(6): 605-610.
- [7] Alam MS, Rahman MM. Dufour and Soret effects on mixed convection flow past a vertical porous flat plate with variable suction. *Nonlinear Analysis: Modelling and Control*. 2006; 11(1): 3-12.
- [8] Afify A. Effects of thermal-diffusion and diffusion thermo on non-Darcy MHD free convective heat and mass transfer past a vertical isothermal surface embedded in a porous medium with thermal dispersion and temperature—dependent viscosity. *Applied Mathematical Modelling*. 2007; 31: 1621-1634.
- [9] Buongiorno J. Convective transport in nano fluids. *J Heat Mass Transfer ASME*. 2006; 128: 240-50.
- [10] Kuznetsov AV, Nield DA. Natural convective boundary-layer flow of a nanofluid past a vertical plate. *Int J Therm Sci*. 2010; 49: 243-7.
- [11] Kamyar A, Saidur R, Hasanuzzaman M. Application of computational fluid dynamics (cfd) for nanofluids. *Int J Heat Mass Transfer*. 2012; 55: 15-6.
- [12] Rana P, Bhargava R. Flow and heat transfer of a nanofluid over a nonlinearly stretching sheet. *Commun Nonlinear Sci Numer Simul*. 2012; 17: 212-26.
- [13] Anbuhezian N, Srinivasan K, Chandrasekaran K, Kandasamy R. Thermophoresis and Brownian motion effects on boundary layer flow of nanofluid in presence of thermal stratification due to solar energy. *Appl Math Mech*. 2012; 33: 765-80.
- [14] Alsaedi A, Awais M, Alsaedi A. Effects of heat generation/absorption on stagnation point flow of nanofluid over a surface with convective boundary conditions. *Commun Nonlinear Sci Numer Simul*. 2012; 17: 4210-23.
- [15] Goyal M, Bhargava R. Numerical study of thermodiffusion effects on boundary layer flow. *Microfluid Nanofluid*. 2014; 17: 591-604.
- [16] Jaber KK. Combined effects of Hall current and variable viscosity on Non-Newtonian MHD flow past a stretching vertical plate. *Journal of Advances in Mathematics*. 2014; 7(3).
- [17] Abdul Gaffar S, Ramachandra Prasad V, Keshava Reddy E. Computational study of non-Newtonian eyringpowell fluid from a horizontal circular cylinder with biot number effects. *International Journal of Mathematical Archive*. 2015; 6(9): 114-132.

- [18] Abdul Gaffar S, Ramachandra Prasad V, Keshava Reddy E. Non-Newtonian thermal convection from an isothermal sphere with Biot number effects. *Int J of Industrial Mathematics*. 2016; 8(2).
- [19] Abdul Gaffar S, Ramachandra Prasad V, Anwar Beg O. Computational study of non-Newtonian Eyring-Powell fluid from a vertical porous plate with Biot number effects. *Journal of the Brazilian Society of Mechanical Sciences and Engineering*. 2017; 39(7): 2747-2765.
- [20] Abdul Hakeema AK, Vishnu Ganesha N, Gangab B. Heat transfer of non-Darcy MHD flow of nano-fluid over a stretching/shrinking surface in a thermally stratified medium with second order slip model. *Scientia Iranica F*. 2015; 22(6): 2766-2784.
- [21] Saeed A, Tassaddiq A, Khan M, Jawad W, Deebani Z, Shah S. Islam Darcy-Forchheimer MHD hybrid nanofluid Flow and heat transfer analysis over a porous stretching cylinder. *Coatings*. 2020; 10(4): 391.
- [22] Chen SS, Leonard R. The axisymmetric boundary layer for a power-law non-Newtonian fluid on a slender cylinder. *Chem Eng J*. 1972; 3: 88-92.
- [23] Lin FN, Chern SY. Laminar boundary layer flow of non-Newtonian fluid. *Int J Heat Mass Transfer*. 1979; 22: 1323-1329.
- [24] Subba Rao A, Amanulla C, Nagendra N, Beg OA, Kadir A. Hydromagnetic flow and heat transfer in a Williamson Non-Newtonian fluid from a Horizontal circular cylinder with Newtonian Heating. *Int J Appl Comput Math*. 2017; 3: 3389-3409.
- [25] Subba Rao A, Nagendra N. Thermal Radiation Effects on Old royd-B Nano fluid from a Stretching Sheet in a non- Darcy porous medium. *Global Journal of Pure and Applied Mathematics*. 2015; 11(2): 45-49.
- [26] Nazar R, Amin N, Pop I. Mixed convection boundary-layer flow from a horizontal circular cylinder with a constant surface heat flux. *Heat Mass Transf*. 2004; 40: 219-227.
- [27] Ibrahim F, Hamad M. Group method analysis of mixed convection boundary-layer flow of a micropolar fluid near a stagnation point on a horizontal cylinder. *Acta Mech*. 2006; 181: 65-81.
- [28] Gorla RSR, El-Kabeir S, Rashad A. Heat transfer in the boundary layer on a stretching circular cylinder in a nanofluid. *J Heat Transf*. 2011; 25: 183-186.
- [29] Chamkha AJ, Rashad A, Aly AM. Transient natural convection flow of a nanofluid over a vertical cylinder. *Meccanica*. 2013; 48: 71-81.
- [30] Rashad A, Chamkha A, Modather M. Mixed convection boundary-layer flow past a horizontal circular cylinder embedded in a porous medium filled with a nanofluid under convective boundary condition. *Comput Fluids*. 2013; 86: 380-388.
- [31] Tlili I, Khan W, Ramadan K. MHD Flow of Nanofluid Flow Across Horizontal Circular Cylinder: Steady Forced Convection. *J Nanofluids*. 2019; 8: 179-186.
- [32] Rashad A, Nabwey HA. Gyrotactic mixed bioconvection flow of a nanofluid past a circular cylinder with convective boundary condition. *J Taiwan Inst Chem Eng*. 2019; 99: 9-17.